Atmos. Chem. Phys. Discuss., 13, 16925–16960, 2013
www.atmos-chem-phys-discuss.net/13/16925/2013/
doi:10.5194/acpd-13-16925-2013


Atmospheric Chemistry and Physics Discussions



# Reactivity of chlorine radical with submicron palmitic acid particles: kinetic measurements and products identification

**M. Mendez[1], R. Ciuraru[1,*], S. Gosselin[1], S. Batut[1], N. Visez[1], and D. Petitprez[1]**

[1]Laboratoire Physicochimie des Processus de Combustion et de l'Atmosphère (PC2A) UMR 8522 CNRS-Université Lille 1, 59655, Villeneuve d'Ascq, France
[*]now at: IRCELYON, Institut de Recherches sur la Catalyse et l'Environnement de Lyon, UMR 5256 CNRS-Université Lyon, Université Lyon 1, 69926 Villeurbanne Cedex, France

Received: 24 April 2013 – Accepted: 9 May 2013 – Published: 25 June 2013

Correspondence to: D. Petitprez (denis.petitprez@univ-lille1.fr)

Published by Copernicus Publications on behalf of the European Geosciences Union.



## Abstract

The heterogeneous reaction of $Cl^{\cdot}$ radicals with sub-micron palmitic acid (PA) particles was studied in an aerosol flow tube in the presence or in the absence of $O_2$. Fine particles were generated by homogeneous condensation of PA vapors and introduced in the reactor where chlorine atoms are produced by photolysis of $Cl_2$ using UV lamps surrounding the reactor. The effective reactive uptake coefficient ($\gamma$) has been determined from the rate loss of PA measured by GC/MS analysis of reacted particles as a function of the chlorine exposure. In the absence of $O_2$, $\gamma = 14 \pm 5$ indicates efficient secondary chemistry involving $Cl_2$. GC/MS analyses have shown the formation of monochlorinated and polychlorinated compounds in the oxidized particles. Although, the PA particles are solid, the complete mass can be consumed. In the presence of oxygen, the reaction is still dominated by secondary chemistry but the propagation chain length is smaller than in the absence of $O_2$ which leads to an uptake coefficient $\gamma = 3 \pm 1$. In the particulate phase, oxocarboxylic acids and dicarboxylic acids are identified by GC/MS. Formation of alcohols and monocarboxylic acids are also suspected. All these results show that solid organic particles could be efficiently oxidized by gas-phase radicals not only on their surface, but also in bulk by mechanisms which are still unclear. Furthermore the identified reaction products are explained by a chemical mechanism showing the pathway of the formation of more functionalized products. They help to understand the aging of primary tropospheric aerosol containing fatty acids.

## 1 Introduction

The concentration of organic matter in marine environments exhibits a seasonal behaviour, which dominates the chemical composition of fine particulate matter during periods of high biological activity (Yoon et al., 2007; O'Dowd et al., 2004; Cavalli et al., 2004; Sciare et al., 2008). Cells of living organisms in the oceans decompose after their death and the hydrophobic cellular constituents accumulate on the water surface

forming a sea-surface micro-layer of 1 to 1000 µm thickness (Hardy, 1982). When sea-salt aerosols (SSA) are generated by the mechanical ejection of droplets from waves and winds, these organic compounds are also ejected, thus becoming a component of the newly formed particles (Barger and Garrett, 1976; Gogou et al., 1998; Marty et al., 1979). Recent laboratory and field measurements have shown that the ratio of the organic mass fraction of SSA increases from 0.1 to near 1 when the ambient aerosol aerodynamic diameter decreases from 1 to 0.1 µm (Keene et al., 2007; Facchini et al., 2008). The exact mechanism for such large organic mass fraction of submicron SSA is not well understood.

Chemical analyses of organic compounds sampled in SSA allowed to identify fatty acid (C12–C18) compounds (Marty et al., 1979), representing up to 10 % in mass of the total organic content of the particles (Mochida et al., 2002).

Molecular characterization of sea-salt aerosol collected in marine air masses shows that fatty acids (FA) consist of relatively short carbon chains (Tervahattu et al., 2002b; Tervahattu et al., 2002a; Mochida et al., 2002; Oros and Simoneit, 2001). Due to the hydrophobic properties of surfactants, the fatty acids are thought to form an organic coating around the inorganic core of the particles (Ellison et al., 1999; Rudich, 2003). When considering a monolayer coating, the surface coverage by FA is estimated to be on the order of 0.3 to 14 % (Tervahattu et al., 2005; Mochida et al., 2002).

Fatty acids are also ubiquitous in airborne particles sampled in urban atmospheres (Oliveira et al., 2007). They are found to contribute to up to 50 % of identified organic compounds from emission sources such as biomass burning (Nolte et al., 2001; Schauer et al., 2001; Fine et al., 2001), cooking (Schauer et al., 2002; He et al., 2004), and automobiles (He et al., 2006). Among the fatty acids, palmitic acid ($C_{16}H_{32}O_2$) is the most abundant one (Mochida et al., 2002).

Recent literature reviews present the physical and chemical processes which occur at the interface of airborne organic particles (Donaldson and Vaida, 2006; Rudich, 2003; George and Abbatt, 2010). Many heterogeneous reactions of atmospheric particles involve the main oxidant of the atmosphere (i.e. the hydroxyl radical $OH^{\cdot}$) which



chemically alters their surfaces thus aging them. The intensity of this aging depends on various parameters such as meteorological conditions, size of the particle, and the chemical composition of the particle surface and bulk. Consequently, the variability of these parameters leads to the observed spatial and temporal variability of the physical and chemical properties of atmospheric aerosols. These heterogeneous processes affect the optical, hygroscopic and reactive properties of airborne particles thereby making uncertain the prediction of their global and regional atmospheric impact. Although the $OH^{\cdot}$ radical is the primary daytime oxidant, halogen atoms (Cl, Br and I) may also significantly participate in oxidation processes, especially in the marine boundary layer (MBL). Halogen species are emitted from anthropogenic sources, but important sources are also represented by the halogen-release from sea-salt aerosols and associated heterogeneous reactions. $Cl^{\cdot}$ atoms are mainly generated from the photolysis of active chlorine species and their concentrations can be up to $10^6$ atom $cm^{-3}$ (Spicer et al., 1998; Pechtl and von Glasow, 2007).

Recent atmospheric measurements (Osthoff et al., 2008) have shown that nitryl chloride ($ClNO_2$) is produced by heterogeneous reactions on sea-salt particles and accumulates during the night. At dawn, the photolysis of nitryl chloride produces a peak of $Cl^{\cdot}$ with an estimated rate of formation of $1 \times 10^6$ atom $cm^{-3}$ $s^{-1}$.

This $Cl^{\cdot}$ atom source seems modest relative to other oxidants. However, it has been reported that $Cl^{\cdot}$ reacts faster than $OH^{\cdot}$ radicals with hydrocarbon compounds (Spicer et al., 1998) and may represent the major oxidant of the troposphere in coastal and industrialized areas, especially at dawn, when concentrations of $OH^{\cdot}$ radicals are low. While sources of reactive halogen species and halogen chemistry in the troposphere are relatively well studied, detailed chemical processes are still unknown (George and Abbatt, 2010).

Given the high reactivity of $Cl^{\cdot}$ atoms with organic compounds and the ubiquity of $Cl^{\cdot}$ and fatty acids in the troposphere, especially in the MBL, it is obvious that this heterogeneous reactivity must be considered. However, only a few experimental studies

between gas-phase radicals ($Cl^{\cdot}$ or $OH^{\cdot}$) with condensed-phase organic compounds, including model organic surfaces, are reported.

Uptake coefficients of $OH^{\cdot}$ on pure palmitic acid (PA) particles between 0.8 and 1 have been reported by McNeill et al. (2008). The authors also measured uptake coefficients for thin PA film coatings on solid and liquid NaCl particles, obtaining lower values than for pure PA experiments (solid, $\gamma_{OH} \approx 0.3$ and liquid, $\gamma_{OH} \approx 0.05$). Experiments with chlorine atoms, generated from $Cl_2$ photolysis, have also been considered as a model for radical-initiated oxidation chemistry which avoids the presence of reactive precursors or side-products during generation of $OH^{\cdot}$. The reactive uptake of $Cl^{\cdot}$ atoms on self-assembled organic monolayers was studied by Moise and Rudich (Moise and Rudich, 2001) using a flow reactor coupled to a chemical ionization mass spectrometer. The uptake coefficient, measured by recording the rate of loss of $Cl^{\cdot}$ radicals, was estimated to be in the range ($0.1<\gamma<1$), close to the diffusion-limited loss rate.

Reactions of $Cl^{\cdot}$ radicals in the presence of $O_2$ have been studied using an aerosol flow tube to stand as a model of the radical-initiated oxidation of liquid phase organic aerosols. In the case of reactions of $Cl^{\cdot}$ radicals with dioctyl sebacate (DOS) particles (Hearn et al., 2007), in the presence of $O_2$, uptake coefficient has been determined by monitoring the rate of loss of DOS species. The uptake coefficient exhibits a value greater than unity ($\gamma_{DOS-OH} = 1.7 \pm 0.3$) indicating a radical chain chemistry. Products were mainly identified in the particles, showing an inefficient volatilization process.

More recently, heterogeneous reactions between $Cl^{\cdot}$ atoms and submicron squalane particles have been investigated in a photochemical aerosol flow tube (Liu et al., 2011). Secondary chain chemistry occurring in the liquid phase has also been demonstrated during these studies. The measured uptake coefficient decreases from a value of ~3 for experiments performed without $O_2$ to a value of 0.65 for experiments in the presence of $O_2$. The product formation in the condensed phase is controlled by competitive reaction rates of $O_2$ and $Cl_2$ with alkyl radicals.

All of these studies about heterogeneous reaction between radical species and organic surfaces or particles as a model for the oxidation of organic aerosols clearly



emphasize the role of $OH^{\cdot}$ or $Cl^{\cdot}$ in initiating oxidation processes *via* an H-abstraction pathway. This is followed by a chain reaction which can accelerate the overall rate of particle transformation. Concerning experiments with $Cl^{\cdot}$ radicals, it is shown that more than 60 % of the initial condensed matter can be consumed by the reactions. Several hypotheses have been put forth to explain these surprising observations: (1) a quite rapid surface renewal process, (2) an efficient secondary chain chemistry in the bulk. These processes might readily occur in the case of liquid droplets (DOS or squalane) but are limited by the diffusion of the species in the liquid phase for both reactants and products. In the case of solid particles, surface renewal can be induced by volatilization. Trapping of species within the particle or phase change of the surface layer cannot be excluded.

Chemical mechanisms adapted from the homogeneous phase have been proposed to interpret the formation of products mainly in the particulate phase but reaction pathways still remain unclear due to the specificity of the condensed phase (microscopic arrangement of the molecules, diffusion process in liquid/solid phase, for example).

We present here of the experimental results of heterogeneous reactivity between $Cl^{\cdot}$ and PA within an Aerosol Flow Tube (AFT) where fine particles generated by homogeneous condensation of PA vapors are introduced with $Cl_2$ as an oxidant precursor. $Cl^{\cdot}$ atoms are generated by photolysis of the molecular chlorine using UV lamps surrounding the reactor. Experiments have been conducted with and without $O_2$. For both cases, uptake coefficients have been determined by monitoring the decay of PA by GC/MS analyses of collected particles on filters at the exit of the reactor. Identification of the reaction products in the condensed phase have been performed by GC/MS analyses and has led to the proposal of a detailed chemical mechanism of the oxidation of carboxylic acids in the particulate matter.

## 2 Experimental section

### 2.1 Aerosol flow tube

An atmospheric pressure aerosol flow tube (AFT) is used to investigate the heterogeneous reactivity of PA particles with chlorine atoms (Fig. 1). The AFT is a 1 m long and 10 cm inner diameter quartz tube surrounded by 8 UV lamps (UVP, 365 BLB, $\lambda_{mean}$ = 365 nm). The particles and gas-phase oxidant precursor are introduced into the upper flange of the reactor through two $\frac{1}{4}''$ stainless connectors. The total flow, monitored by mass flowmeters, is fixed at 4.0 L min$^{-1}$ which corresponds to a mean residence path time of 180 s in the AFT.

### 2.2 Reactant generation

Palmitic acid (≥98 %) is purchased from Roth. Chemicals purchased from Aldrich are: dichloromethane (99.8 %). Chemicals from Fluka are: tetradecane (≥98 %), hexadecane (≥98 %). N, O-Bis (trimethylsilyl) trifluoroacetamide, $C_8H_{18}F_3NOSi_2$-Trimethylchlorosilane (BSTFA-TMCS) (99 %–1 %) solution is purchased from Supelco. Gases are purchased from Praxair: Synthetic air 3.0, Nitrogen 4.6. Chlorine (1 % of $Cl_2$ in Helium) is purchased from Air Liquide (99.6 %).

### 2.3 Particle generation

Palmitic acid particles are generated by homogeneous nucleation in a stream of 1 L min$^{-1}$ $N_2$ or $N_2/O_2$ flowing through a glass vessel containing 5 grams of PA. An heating wire wraps the glass vessel and the PA temperature is kept constant (±1 °C) using a temperature controller. The flow is diluted with 1 L min$^{-1}$ of $N_2$ or $N_2/O_2$ and sent to a condensation tube of 1.5 L volume at room temperature. The size distribution of the particles is continuously recorded by a SMPS (model TSI 3080L) every 2 min. Palmitic acid particle density was assumed to be the liquid phase density



($d$ = 0.853 g cm$^{-3}$). Depending on temperature and flows, mass concentrations between 500 and 1000 µg m$^{-3}$ of PA particles are generated. For a temperature of around 120 °C, the setup produces a log-normal particle size distribution with a mean surface-weighted diameter of ∼500 nm and a geometric standard deviation of ∼1.5. Measuring the aerosol concentration before and after the AFT reveals that the mean diameter is not modified and that at maximum a mass loss of 10 % occurred while passing through the AFT.

### 2.4 Atomic chlorine production

Chlorine radicals are generated along the length of the AFT by powering all or some of the 8 UV lamps. The Cl concentration can also be adjusted by controlling the $Cl_2$ initial concentration in the AFT.

Chlorine radical concentration was measured by performing reference kinetic experiments with acetone. Molecular chlorine (3 to 20 ppm) and acetone (50 ppm) are introduced in the reactor and the reaction between acetone and Cl takes place with a second order rate constant ($k_{ref}$) of 2.09 × 10$^{-12}$ cm$^3$ molec$^{-1}$ s$^{-1}$ (Liu et al., 2011; George et al., 2007). The loss of acetone is monitored by Fourier transform infrared (FTIR) spectroscopy by integration of the absorbance of the C-C stretching band at 1217 cm$^{-1}$ (Perelygin and Klimchuk, 1974) between 1160 and 1260 cm$^{-1}$. The loss rate of acetone can be expressed as:

$$v = \frac{d[\text{Acet}]}{dt} = -k_{ref}[\text{Acet}][Cl] \quad (1)$$

Integration of Eq. (1) leads to the determination of the chlorine exposure ($\langle Cl \rangle_t$.t in atom cm$^{-3}$ s) which is the product of the reaction time t with the time averaged chlorine

radical concentration along the reactor $\langle Cl \rangle_t$:

$$\frac{\ln \frac{[\text{Acet}]_t}{[\text{Acet}]_0}}{-k_{\text{ref}}} = \int_0^t [Cl]\,dt = \langle Cl \rangle_t \cdot t \tag{2}$$

where $[\text{Acet}]_0$ and $[\text{Acet}]_t$ are the initial and final concentrations of acetone measured by FTIR spectroscopy respectively. As shown in Fig. 2, the chlorine exposure, $\langle Cl \rangle_t \cdot t$, is proportional to $[Cl_2]$ with a maximum time averaged chlorine concentration of 2.25 $10^9$ atom cm$^{-3}$. The ratio $[Cl_2]/[Cl^{\cdot}]$ expresses the photodissociation efficiency and is greater than 3000 and means that on average one $Cl_2$ out of 6000 is dissociated by photolysis and produces 2 $Cl^{\cdot}$ radicals.

### 2.5 Analytical procedure

#### 2.5.1 Particle sampling and GC/MS analysis

At the reactor outlet, the particles are sampled on a PTFE (PolyTetraFluoroEthylene) filter (Millipore FALP, 1.0 µm, diameter 47 mm) for 10 min in order to collect about 20 µg of PA. The filter is then placed in a 1.5 mL vial and 10 µL of a solution containing two internal standards (tetradecane and hexadecane) and 25 µL of a commercial mixture 99 % BSTFA/1 % TMCS are deposited directly on the membrane. Quantitative analysis of carboxylic acids by gas chromatography requires derivatization of the –COOH function. Silylation by BSTFA (N, O-Bis (trimethylsilyl) trifluoroacetamide, $C_8H_{18}F_3NOSi_2$) has been previously used for the determination of mono- and dicarboxylic acids in samples of atmospheric particles collected on filters (Docherty and Ziemann, 2001; Wang et al., 2009; Zuo et al., 2007; Yu et al., 1998). Trimethylchlorosilane (TMCS) acts as a catalyst by increasing the silyl donor strength of the BSTFA. After finally adding a volume of 1 mL of dichloromethane, the filter is subjected to 10 min of sonification. For product identification, only a volume of 200 µL of dichloromethane is added before the



sonification. NIST mass spectra database (V2.2) is used for identification. After the extraction and sylilation steps, 1 µL of the solution is injected in a Gas Chromatograph Mass Spectrometer (Perkin-Elmer GC Clarus 680). Chromatographic conditions are as follows: inlet 250 °C, split mode 5 mL min$^{-1}$, constant column flow 1 mL min$^{-1}$, oven temperature: 50 °C for 0.5 min, ramp +20 °C min$^{-1}$ to the final temperature 310 °C. Separation is provided by an Elite-5MS 30 meter long column (diameter 250 µm and film thickness 0.5 µm). Identification and quantification is performed on a Clarus 600C mass spectrometer in 70 eV electron impact mode with a source temperature of 180 °C.

Quantification of palmitic acid is done by injecting standard solution of known concentration. The ion fragment corresponding to the sylil group $Si(CH_3)_3$ ($m/z = 73$) is chosen for the quantification of sylilated palmitic acid. All samples are injected in triplicates in SIM mode for the quantification and once in scan mode for identification. The mass of PA particles collected on filter for 10 min was quantified by GC/MS and compared to the mass concentration measured by the SMPS analyses during the same period. It appears that the mass derived from GC/MS represents 80 %±10 % of the mass as determined by the SMPS.

#### 2.5.2 FTIR analysis

Gas phase analyses were performed by Fourier transform infrared spectroscopy (FTIR). The FTIR spectra are recorded with an Avatar–Thermo Scientific spectrometer equipped with a 10 m length multipath cell. Each spectrum is obtained while averaging 100 scans in the 400–4000 cm$^{-1}$ spectral range with a spectral resolution of 1 cm$^{-1}$. Background spectra are taken before and after reactivity experiments to make sure that measured products are not stuck on the mirrors of the cell.

## 3 Results and discussion

### 3.1 Chlorine reactivity in $N_2$

#### 3.1.1 Kinetic measurements

First, we studied the heterogeneous oxidation of palmitic acid particles by Cl· radicals in an $O_2$-free environment. Classical parameter determined in heterogeneous kinetic measurements is the reactive uptake coefficient $\gamma_{Cl}$ which is defined as the fraction of Cl collisions with the particle leading to the loss of Cl in the gas-phase. Since the loss of Cl is not measured in this experiment, the reaction is monitored through the reactive loss of palmitic acid in the particle phase $\gamma_{PA}$. The PA loss rate can be expressed as follows:

$$\frac{d[\mathrm{PA}]}{dt} = -k_{\mathrm{PA}}[\mathrm{Cl}][\mathrm{PA}] \tag{3}$$

where $k_{PA}$ ($cm^3\,molec^{-1}\,s^{-1}$) is the second order rate constant of the reaction of PA with Cl·. [PA] and [Cl] are the time dependent concentrations of the reactants ($molec\,cm^{-3}$). The palmitic loss $\phi_{loss}$ is defined by:

$$\phi_{\mathrm{loss}} = \frac{V}{S_P} k_{\mathrm{PA}}[\mathrm{Cl}][\mathrm{PA}] \tag{4}$$

where $S_P$ is the particle surface density ($cm^2\,cm^{-3}$) and $V$ the volume of the particle. The flux of collisions $\varphi_{coll}$ occurring on the particle surface per second is expressed in the Eq. (5):

$$\phi_{\mathrm{coll}} = \frac{[Cl]\cdot\omega_{\mathrm{Cl}}}{4} \tag{5}$$



where $\omega_{Cl}$ is the mean speed of gas-phase Cl ($cm\,s^{-1}$). The integration of Eq. (3) leads to:

$$k_{\mathrm{PA}} = \frac{\ln \frac{[\mathrm{PA}]_0}{[\mathrm{PA}]_t}}{\langle \mathrm{Cl} \rangle_t \cdot t}$$

$[PA]_0$ and $[PA]_t$ are the initial and final concentrations of particle-phase PA, respectively, and measured by GC/MS ($molec\,cm^{-3}$). $\langle Cl \rangle_t$.t ($atom\,cm^{-3}\,s$) is the exposure obtained by the reference kinetics measurements and $k_{PA}$ is experimentally determined from the decay of palmitic acid as a function of the exposure. Moreover, $[PA]_0$ can be replaced in the uptake coefficient expression by:

$$[\mathrm{PA}]_0 = \frac{V_P \cdot \rho_{\mathrm{PA}} \cdot N_A}{M_{\mathrm{PA}}} \tag{6}$$

where $V_P$ is the particle volume density ($cm^3\,cm^{-3}$), $M_{PA}$ is the molar mass of palmitic acid ($M_{PA} = 256\,g\,mol^{-1}$), $\rho_{PA}$ is the palmitic acid density ($\rho_{PA} = 0.853\,g\,cm^{-3}$) and $N_A$ is the Avogadro's number. Finally, the uptake coefficient $\gamma_{PA}$can be expressed as:

$$\gamma_{\mathrm{PA}} = \frac{\phi_{\mathrm{loss}}}{\phi_{\mathrm{coll}}} = \frac{4 \cdot k_{\mathrm{PA}} \cdot D_{\mathrm{mean}} \cdot \rho_{\mathrm{PA}} \cdot N_A}{\omega_{\mathrm{Cl}} \cdot 6 \cdot M_{\mathrm{PA}}} \tag{7}$$

$D_{mean}$ is the mean surface-weighted diameter of the particle distribution and is calculated by $V_P/S_P = D_{mean}/6$ (Smith et al., 2009). The mean particle diameter is determined by SMPS measurements and is assumed constant and equal to the initial mean particle diameter.

The normalized decay of ($[PA]_t/[PA]_0$) as a function of Cl· exposure is shown in Fig. 3. The decay constant $k_{PA}$ is obtained from an exponential fit to the experimental measurements for exposure ranging from 0 to $4 \times 10^{11}$ $atom\,molec\,cm^{-3}\,s$.

Using the rate constant $k_{PA}$ obtained from the exponential fit of kinetic data in Fig. 3, the initial uptake coefficient $\gamma_{PA}$ has been determined to be equal to 14±5 in an oxygen-free environment. Using the formalism developed by Fuchs and Sutugin, 1970, the calculation of the gas-phase diffusion limitation leads to a small correction of $\gamma$ which is significantly smaller than the total error form the experiment setup. The high value of $\gamma$ means that: (1) the heterogeneous reaction of PA with $Cl^{\cdot}$ radical is very efficient; (2) the secondary chemistry is leading the overall reaction. These results are similar to those of Liu et al., 2011 who reported $\gamma = 3$ for the uptake coefficient of chlorine on squalane particles. However, Liu et al. determined the loss of squalane as a function of the total chlorine radical concentration while, in this study, the loss of palmitic acid is measured as a function of the chlorine radical concentration produced from the photolysis of $Cl_2$. As a result, the uptake coefficients cannot be strictly compared but both show the importance of secondary chemistry.

By definition, the initial uptake coefficient, when derived from the measurement of the rate loss of the gas phase oxidant $Cl_g$, $\gamma_{Cl,}$ cannot be greater than 1. Here the uptake coefficient, determined from the rate loss of the condensed phase ($\gamma_{PA}$) is significantly greater than one ($\gamma_{PA} = 14 \pm 5$), indicating an efficient secondary heterogeneous chemistry leading the whole reaction. The chain propagation length is the ratio between the number of palmitic acid molecules lost and $Cl_g$ atoms that react and corresponds to the ratio $\gamma_{PA}/\gamma_{Cl}$. The chain propagation length is at least equal to 14.

### 3.1.2 Reaction mechanism

The high value of the uptake coefficient confirms that the PA consumption is enhanced by secondary chemistry. Liu et al. proposed a catalytic mechanism which can be adapted to our oxidation process.

$$Cl_2 \rightarrow Cl^{\cdot}_g + Cl^{\cdot}_g \qquad Cl_2 \text{photolysis} \qquad \text{(R0)}$$



$$RH + Cl^{\cdot}_g \rightarrow R^{\cdot} + HCl \qquad \text{H-Abstraction} \qquad \text{(R1)}$$

$$R^{\cdot} + Cl_2 \rightarrow RCl + Cl^{\cdot}_p \qquad Cl_2 \text{ addition} \qquad \text{(R2)}$$

$$RH + Cl^{\cdot}_p \rightarrow R^{\cdot} + HCl \qquad \text{Second H-abstraction} \qquad \text{(R3)}$$

$$R^{\cdot} + Cl^{\cdot}_p \rightarrow RCl \qquad \text{Termination reaction} \qquad \text{(R4)}$$

$$R^{\cdot} + Cl^{\cdot}_g \rightarrow RCl \qquad \text{Termination reaction} \qquad \text{(R5)}$$

$$Cl^{\cdot} + Cl^{\cdot} + M \rightarrow Cl_2 + M \qquad \text{Termination reaction} \qquad \text{(R6)}$$

$Cl^{\cdot}_g$ is defined as a gas phase $Cl^{\cdot}$ produced from the $Cl_2$ photolysis. The initiation Reaction R1 is the heterogeneous reaction between $Cl^{\cdot}_g$ and particle-phase PA at the surface of the particle producing an alkyl radical $R^{\cdot}$. A chlorine molecule can be added on the $R^{\cdot}$ leading to the formation of a chlorinated product and atomic chlorine $Cl^{\cdot}_g$. This chlorine atom is released from the surface of the particle and can easily react with another hydrocarbon. R4, R5 and R6 are possible reactions terminating the radical chain propagation. R6 could occur heterogeneously via the collision between $Cl^{\cdot}_g$ and $Cl^{\cdot}_p$ but also can take place in the condensed phase and involve two $Cl^{\cdot}_p$. Such heterogeneous mechanism has already been observed in previous studies performed either on NaCl particles (Ciuraru et al., 2011) or on ammonium sulphate particles (Ciuraru et al., 2012). The reaction rate of R1 is defined by the uptake coefficient of chlorine on the particle surface $\gamma_{Cl}$. R2 is a source of $Cl^{\cdot}$ allowing the chlorine concentration to be renewed; ($[Cl_2]/[Cl^{\cdot}] > 3000$).

### 3.1.3 Change of the particle size distribution

The SMPS data indicate that the initial log-normal particle distribution mean diameter shifts from 520 to 405 nm after a Cl-exposure of $1.25 \times 10^{11}$ atom cm$^{-3}$ s (see Fig. 4). For this specific exposure, the aerosol mass measured by SMPS decreases by 40 % whereas the GC/MS analysis shows that 80 % of the particle-phase PA is lost. Chlorinated products have a higher molar mass than PA and it is assumed that they remain in the condensed phase, thus changing the density of oxidised particles compared to initial pure PA particles. The oxidized particle diameter cannot therefore be rigorously determined because the SMPS mean particle diameter is obtained from the electrical mobility of the particle which depends on the density. Assuming that the change of the mean diameter is only due to the density variation would indicates that the particle density would have increase from 0.853 to 1.850. This value seems to be high for an organic compound and suggests that the mean diameter change is also due to the volatilization of products. For this reason, the initial mean surface-weighted particle diameter is considered in this following kinetic study.

### 3.1.4 Particulate-phase products identification

Evidence of the presence of monochlorinated palmitic acid is found in the mass spectra. Fragments with $m/z = 362$ and 364 are detected and correspond to the parent peaks of the silylated monochlorinated palmitic acid ($C_{15}H_{30}Cl$-COO-Si-$(CH_3)_3$) with characteristic pattern for the $m/z = 35$ and 37 isotopic relative abundances of chlorine. In those mass spectra, the presence of the peak $m/z = 117$ (corresponding to -COO-Si-$(CH_3)_3$) shows that the carboxylic acid function has not been modified and the chlorine atom has not been added on the oxygen atom. Because the hydrogen abstraction by chlorine can occur at different sites, several monochlorinated products are detected instead of one main product.

Dichlorinated palmitic acid molecules are also detected in the sampled particles. The multiplication of different constitutional isomers induces much smaller peaks than



the monochlorinated ones. The mass spectra of those species show the $m/z = 396$, 398 and 400 amu, indicating the presence of the parent peak of $C_{15}H_{29}Cl_2$-COO-Si-$(CH_3)_3$ with the natural abundance of isotopic species. The mass spectra of those species indicate the presence of the silylated monochlorinated palmitic acid fragment ($m/z = 362$ and 364) and also the silylated carboxylic acid function. Polychlorinated palmitic acid molecules such as trichlorinated palmitic acid molecules and more are highly suspected but the signal/noise ratios are too low to get unambiguous identifications.

## 3.2 Chlorine reactivity in the presence of $O_2$

### 3.2.1 Kinetic measurements

The effect of oxygen on the heterogeneous reactivity between Cl$^{\cdot}$ atoms and PA particles has been explored by using a $N_2/O_2$ mixture (80 %/20 %) as a carrier gas for the aerosol flow. The particle-phase PA decay is much slower when oxygen is added in the chemical system compared to the measurements without $O_2$ (see Fig. 5). The uptake coefficient of $\gamma_{PA}$,= 3 has been determined and shows that the catalytic secondary reactions still govern the decay of PA but the propagation length of the catalytic reactions is reduced. The decrease of the uptake coefficient as function of the oxygen concentration has been previously observed by Liu et al., 2011 in the heterogeneous oxidation of squalane by chlorine radicals. The secondary chemistry involving $Cl_2$ is considered as insignificant because the ratio between $O_2$ and $Cl_2$ concentrations is greater than 1,000. In the presence of $O_2$, a new reaction (R$^{\cdot}$ + $O_2$) competes with R2, leading to the formation of an alkyl peroxy radical instead of a chlorinated radical.

### 3.2.2 Particulate products identification

The products identification has been performed after the derivatization step by collecting the particles at the AFT outlet during 30 min (see Fig. 6). We were not able to identify any products on non-derivatized samples.

The main identified products are dicarboxylic acids and oxocarboxylic acids and confirm the observations by McNeill (McNeill et al., 2008) where ketoacids were detected. This new study allows to identify and speciate dicarboxylic and oxocarboxylic acids. Oxocarboxylic acids detected are oxopentanoic, oxohexanoic and oxoheptanoic acid.

The chromatogram shows that the oxocarboxylic acids are obtained by fragmentation of the palmitic acid but the C=O function position could not be determined in the mass spectra. Moreover, we suppose that several isomers of oxocarboxylic acids can be produced and that they may have not been separated with the gas chromatography conditions. Dicarboxylic acids have been detected from the propanedioic acid (C3) to octanedioic acid (C8). The normalized yields (Fig. 7) are calculated from the ratio of chromatographic peak areas assuming that the response coefficients are equal. The normalized yields of the detected dicarboxylic acids decrease as a function of the chain carbon length (Fig. 7). For that reason, oxalic acid is suspected to be produced but its retention time is too low to allow a clear detection under our chromatographic conditions.

The presence of minor products with alcohol functions is suspected: hydroxyethanoic acid, hydroxypropanoic acid and hexanediol which are consistent with the formation of hydroxyacid proposed by McNeill et al., 2008. Monocarboxylic acids have also been detected in much lower quantities. Moreover, the gas-phase products HCl, $CO_2$ and CO have been clearly identified by FTIR spectroscopy by means of their characteristic fundamental bands.



### 3.2.3 Chemical mechanism

We propose a reaction mechanism (see Fig. 8) for the radical initiated oxidation of PA particles adapted from the mechanism presented by George and Abbatt (George and Abbatt, 2010). We have intentionally reduced the reaction mechanism to the observed pathways based on the identified products. Because no relative carbon yields are suggested in our study, we cannot determine which reaction path dominates. Nevertheless, this reaction mechanism summarizes the observed reaction pathways and products of the radical initiated oxidation of palmitic acid under our experimental conditions.

As in the case of the experiments performed without $O_2$, R1 leads to the abstraction of a hydrogen atom by a $Cl^{\cdot}$ radical from the aliphatic chain or from the carboxylic acid group (Smith and Ravishankara, 2002; Singleton et al., 1989). R7 is the internal recombination of $RCOO^{\cdot}$ to form $CO_2$ and the $R^{\cdot}$ radical. R8 leads to the formation of monocarboxylic acids in the case of internal recombination. If $RCOO^{\cdot}$ reacts with another RH molecule, the products formed are the $R^{\cdot}$ radical and the palmitic acid. The $R^{\cdot}$ radicals react with $O_2$ to from $RO_2^{\cdot}$ radicals. On the other hand, if an internal recombination occurs, it leads to form a monocarboxylic acid with a carbon chain length smaller than the palmitic acid and the $R^{\cdot}$ radical including the remaining carbon chain. This latter will also react with $O_2$ to form new products as well as the $R^{\cdot}$ radical formed by R7.

R10 shows the recombination of $RO_2^{\cdot}$ with R'H to form a dicarboxylic acid, an alkane and a hydrocarbon radical. This reaction may also occur by internal recombination and lead to the formation of a dicarboxylic acid and a hydrocarbon radical. R11 leads to the formation of oxo-carboxylic acids by recombination of two $RO_2^{\cdot}$ radicals. This recombination can also produce an oxo-carboxylic acid and an alcohol as shown in R12.

The current study suggests that those species can also be produced by the radical-initiated oxidation of carboxylic acids. Moreover, the same compounds should be expected independent of the radical ($OH^{\cdot}$ or $Cl^{\cdot}$) that is involved in the H abstraction.

## 4 Conclusions and atmospheric implications

Kinetic studies have been performed to measure the uptake coefficient of chlorine atom on palmitic acid particles as a function of chlorine exposure formed by photolysis of $Cl_2$. The uptake coefficient has been derived from two experimental conditions (with and without $O_2$) by measuring the palmitic acid lost from the particle phase as a function the chlorine exposure. First, we have realized these experiments in an oxygen free environment. In this case, the uptake coefficient $\gamma_{PA}$ is estimated to be $\gamma = 14 \pm 5$. Secondly, we determined the uptake coefficient in a $N_2/O_2$ mixture (80/20). It appears that palmitic acid loss rate as a function of the chlorine exposure is lower and $\gamma_{PA} = 3 \pm 1$. It must be considered that the chlorine exposure has been defined as the exposure to the chlorine atom form by photolysis of $Cl_2$ only and measured during separate experiments. Contrariwise, in the work of Hearn et al. and Liu et al., reference kinetic study were performed simultaneously with the particle oxidation and considered all the $Cl^{\cdot}$ atoms formed during the experiments. The uptake coefficient determined in those studies cannot be compared directly with the uptake coefficients measured in this work. Under the conditions in this study, their uptake coefficient would have been greater. However, the general behaviour is similar: (1) the uptake coefficient variation is a function of $O_2$ concentration; (2) the uptake coefficient greater than 1 explained by a secondary chemistry involving radicals $R^{\cdot}$.

The heterogeneous reactivity experiments we performed without $O_2$ reveal that: (1) an important secondary chemistry where $Cl_2$ is involved; (2) monochlorinated and polychlorinated compounds are formed (from $PACl_1$ to $PACl_4$ detected). Although, the palmitic acid particles are solid, the complete palmitic acid mass can be consumed. This behaviour has already been observed for heterogeneous chemistry involving liquid compound where diffusion of compounds and products in the bulk can be suggested as an explanation for fast refreshing of the surface. In the case of solid particles, this surprising observation is somehow more difficult to discuss. Two hypotheses can be put forward: (1) an efficient volatilization of the products formed at the surface of the



particle or, (2) a phase change of the first layers facilitating diffusion or trapping of the compounds within the particle (McNeill et al., 2008; Marcolli et al., 2004; Garton et al., 2000).

In the presence of oxygen, the reaction is still dominated by secondary chemistry but the propagation chain length is smaller than in the absence of $O_2$ because there is no regeneration of $Cl^{\cdot}$. Those results confirm the observation made by Liu et al. (Table 1) for squalane (Sq) but are in disagreement with the Hearn and Smith study which reports that the rate of DOS loss is faster in the presence of oxygen. The absolute values of $\gamma$ determined in this work for $Cl^{\cdot}$ + PA are significantly higher than for $Cl^{\cdot}$ + Sq. As detailed before, it is difficult to compare these values because $\gamma$ values have been determined in two different ways by the authors. However, the effect of adding oxygen to the system is the same in both cases. Indeed, the uptake coefficient decreases by a factor of five when oxygen is added to the chemical system.

Results of experiments with $O_2$ allow us to identify products relevant to the detected compounds in the atmospheric particles. We have observed the formation of HCl, CO and $CO_2$ in the gas-phase, while, in the particle-phase, oxocarboxylic acids and dicarboxylic acids are detected. Alcohols and monocarboxylic acids are also suspected. Dicarboxylic and oxocarboxylic acids have been measured in the particulate matter by several field measurement campaigns (Kawamura and Gagosian, 1987; Kawamura and Gagosian, 1990; Kawamura and Ikushima, 1993; Mochida et al., 2002; Kawamura and Yasui, 2005; Wang et al., 2006; S. Kundu, 2010; Pavuluri et al., 2010; Hegde and Kawamura, 2012; Mkoma and Kawamura, 2013) in a large number of environmental conditions (urban, costal, remote marine, remote continental). The presence of oxocarboxylic acids is explained by biomass combustion and the aging of primary organic matter (Kawamura and Gagosian, 1987; Kawamura and Gagosian, 1990; Kawamura and Yasui, 2005; Kundu, 2010; Pavuluri et al., 2010; Hegde and Kawamura, 2012; Mkoma and Kawamura, 2013). In this study, we observed that the concentration of the dicarboxylic acids decreases with the carbon chain length. Similar distributions of dicarboxylic acids have been observed several times in ambient times in ambient particulate

matter in field measurements campaigns of particulate organic matter (Kawamura and Yasui, 2005; Kundu, 2010; Pavuluri et al., 2010; Hegde and Kawamura, 2012; Mkoma and Kawamura, 2013). Those studies correlate the presence of dicarboxylic acids with the oxidation of fatty acids and show that oxalic acid is the main dicarboxylic acid whatever the origin of the analyzed samples. Those conclusions suggest that a large amount of oxalic acid is formed in our experimental system.

Finally, we have highlighted that there is a significant fragmentation and functionalization of the fatty acids by oxidation initiated by radicals. This leads to the volatilization of oxygenated low-molecular weight organic compounds in the atmosphere. Moreover, the functionalization of the primary organic matter leads to the formation of more polar compounds at the surface of the particle and suggests a modification of the hygroscopic properties of the particle. As fatty acids are the most abundant organic compounds in the marine aerosols, the aging process of those particles via radical-initiated chemistry may facilitate cloud droplet activation (Westervelt et al., 2012).

## References


Barger, W. R. and Garrett, W. D.: Surface Active Organic Material in Air Over the Mediterranean and Over the Eastern Equatorial Pacific, J. Geophys. Res., 81, 3151–3157, doi:10.1029/JC081i018p03151, 1976.

Cavalli, F., Facchini, M. C., Decesari, S., Mircea, M., Emblico, L., Fuzzi, S., Ceburnis, D., Yoon, Y. J., O'Dowd, C. D., Putaud, J. P., and Dell'Acqua, A.: Advances in characterization of size-resolved organic matter in marine aerosol over the North Atlantic, J. Geophys. Res., 109, D24215, doi:10.1029/2004jd005137, 2004.

Ciuraru, R.: Étude de la réactivite du chlore atomique avec des particules d'aérosols d'intérêt atmosphérique, 2010.

Ciuraru, R., Gosselin, S., Visez, N., and Petitprez, D.: Heterogeneous reactivity of chlorine atoms with sodium chloride and synthetic sea salt particles, Phys. Chem. Chem. Phys., 13, 19460–19470, 2011.





Ciuraru, R., Gosselin, S., Visez, N., and Petitprez, D.: Heterogeneous reactivity of chlorine atoms with ammonium sulfate and ammonium nitrate particles, Phys. Chem. Chem. Phys., 14, 4527–4537, 2012.

Docherty, K. S. and Ziemann, P. J.: On-line, inlet-based trimethylsilyl derivatization for gas chromatography of mono- and dicarboxylic acids, J. Chromatogr. A, 921, 265–275, doi:10.1016/s0021-9673(01)00864-0, 2001.

Donaldson, D. J. and Vaida, V.: The Influence of Organic Films at the Air-Aqueous Boundary on Atmospheric Processes, Chem. Rev., 106, 1445–1461, doi:10.1021/cr040367c, 2006.

Ellison, G. B., Tuck, A. F., and Vaida, V.: Atmospheric processing of organic aerosols, J. Geophys. Res., 104, 11633–11641, doi:10.1029/1999jd900073, 1999.

Facchini, M. C., Rinaldi, M., Decesari, S., Carbone, C., Finessi, E., Mircea, M., Fuzzi, S., Ceburnis, D., Flanagan, R., and Nilsson, E. D.: Primary submicron marine aerosol dominated by insoluble organic colloids and aggregates, Geophys. Res. Lett., 35, L17814, 2008.

Fine, P. M., Cass, G. R., and Simoneit, B. R.: Chemical characterization of fine particle emissions from fireplace combustion of woods grown in the northeastern United States, Environ. Sci. Technol., 35, 2665–2675, 2001.

Fuchs, N. and Sutugin, A.: High-dispersed aerosols, Ann Arbor Science Publishers, 1970.

Garton, D. J., Minton, T. K., Alagia, M., Balucani, N., Casavecchia, P., and Volpi, G. G.: Comparative dynamics of Cl (P) and O (P) interactions with a hydrocarbon surface, J. Chem. Phys., 112, 5975–5985, 2000.

George, I. J. and Abbatt, J. P. D.: Heterogeneous oxidation of atmospheric aerosol particles by gas-phase radicals, Nat. Chem., 2, 713–722, 2010.

George, I. J., Vlasenko, A., Slowik, J. G., Broekhuizen, K., and Abbatt, J. P. D.: Heterogeneous oxidation of saturated organic aerosols by hydroxyl radicals: uptake kinetics, condensed-phase products, and particle size change, Atmos. Chem. Phys., 7, 4187–4201, doi:10.5194/acp-7-4187-2007, 2007.

Gogou, A. I., Apostolaki, M., and Stephanou, E. G.: Determination of organic molecular markers in marine aerosols and sediments: one-step flash chromatography compound class fractionation and capillary gas chromatographic analysis, J. Chromatogr. A, 799, 215–231, doi:10.1016/s0021-9673(97)01106-0, 1998.

Hardy, J. T.: The sea surface microlayer: Biology, chemistry and anthropogenic enrichment, Prog. Oceanogr., 11, 307–328, doi:10.1016/0079-6611(82)90001-5, 1982.

He, L.-Y., Hu, M., Huang, X.-F., Yu, B.-D., Zhang, Y.-H., and Liu, D.-Q.: Measurement of emissions of fine particulate organic matter from Chinese cooking, Atmos. Environ., 38, 6557–6564, doi:10.1016/j.atmosenv.2004.08.034, 2004.

He, L.-Y., Hu, M., Huang, X.-F., Zhang, Y.-H., and Tang, X.-Y.: Seasonal pollution characteristics of organic compounds in atmospheric fine particles in Beijing, Sci. Total Environ., 359, 167–176, 2006.

Hearn, J. D. and Smith, G. D.: A mixed-phase relative rates technique for measuring aerosol reaction kinetics, Geophys. Res. Lett., 33, L17805, doi:10.1029/2006gl026963, 2006.

Hearn, J. D., Renbaum, L. H., Wang, X., and Smith, G. D.: Kinetics and products from reaction of Cl radicals with dioctyl sebacate (DOS) particles in $O_2$: a model for radical-initiated oxidation of organic aerosols, Phys. Chem. Chem. Phys., 9, 167–176, 2007.

Hegde, P., and Kawamura, K.: Seasonal variations of water-soluble organic carbon, dicarboxylic acids, ketoacids, and α -dicarbonyls in the central Himalayan aerosols, Atmos. Chem. Phys. Discuss., 12, 935–982, doi:10.5194/acpd-12-935-2012, 2012.

Kawamura, K. and Gagosian, R. B.: Implications of [omega]-oxocarboxylic acids in the remote marine atmosphere for photo-oxidation of unsaturated fatty acids, Nature, 325, 330–332, 1987.

Kawamura, K., and Gagosian, R. B.: Mid-chain ketocarboxylic acids in the remote marine atmosphere: Distribution patterns and possible formation mechanisms, J. Atmos. Chem., 11, 107–122, doi:10.1007/bf00053670, 1990.

Kawamura, K.chain propagation length and Ikushima, K.: Seasonal changes in the distribution of dicarboxylic acids in the urban atmosphere, Environ. Sci. Technol., 27, 2227–2235, doi:10.1021/es00047a033, 1993.

Kawamura, K. and Yasui, O.: Diurnal changes in the distribution of dicarboxylic acids, ketocarboxylic acids and dicarbonyls in the urban Tokyo atmosphere, Atmos. Environ., 39, 1945–1960, doi:10.1016/j.atmosenv.2004.12.014, 2005.

Keene, W. C., Maring, H., Maben, J. R., Kieber, D. J., Pszenny, A. A., Dahl, E. E., Izaguirre, M. A., Davis, A. J., Long, M. S., and Zhou, X.: Chemical and physical characteristics of nascent aerosols produced by bursting bubbles at a model air-sea interface, J. Geophys. Res., 112, D21202, doi:10.1029/2007JD008464, 2007.

Liu, C.-L., Smith, J. D., Che, D. L., Ahmed, M., Leone, S. R., and Wilson, K. R.: The direct observation of secondary radical chain chemistry in the heterogeneous reaction



of chlorine atoms with submicron squalane droplets, Phys. Chem. Chem. Phys., 13, doi:10.1039/C1CP20236G, 2011.

Marcolli, C., Luo, B., and Peter, T.: Mixing of the organic aerosol fractions: Liquids as the thermodynamically stable phases, J. Phys. Chem. A, 108, 2216–2224, 2004.

Marty, J. C., Saliot, A., Buat-Ménard, P., Chesselet, R., and Hunter, K. A.: Relationship Between the Lipid Compositions of Marine Aerosols, the Sea Surface Microlayer, and Subsurface Water, J. Geophys. Res., 84, 5707–5716, doi:10.1029/JC084iC09p05707, 1979.

McNeill, V. F., Yatavelli, R. L. N., Thornton, J. A., Stipe, C. B., and Landgrebe, O.: Heterogeneous OH oxidation of palmitic acid in single component and internally mixed aerosol particles: vaporization and the role of particle phase, Atmos. Chem. Phys., 8, 5465–5476, doi:10.5194/acp-8-5465-2008, 2008.

Mkoma, S. L. and Kawamura, K.: Molecular composition of dicarboxylic acids, ketocarboxylic acids, $\alpha$-dicarbonyls and fatty acids in atmospheric aerosols from Tanzania, East Africa during wet and dry seasons, Atmos. Chem. Phys., 13, 2235–2251, doi:10.5194/acp-13-2235-2013, 2013.

Mochida, M., Kitamori, Y., Kawamura, K., Nojiri, Y., and Suzuki, K.: Fatty acids in the marine atmosphere: Factors governing their concentrations and evaluation of organic films on sea-salt particles, J. Geophys. Res., 107, 4325, doi:10.1029/2001jd001278, 2002.

Moise, T. and Rudich, Y.: Uptake of Cl and Br by organic surfaces – A perspective on organic aerosols processing by tropospheric oxidants, Geophys. Res. Lett., 28, 4083–4086, doi:10.1029/2001gl013583, 2001.

Nolte, C. G., Schauer, J. J., Cass, G. R., and Simoneit, B. R.: Highly polar organic compounds present in wood smoke and in the ambient atmosphere, Environ. Sci. Technol., 35, 1912–1919, 2001.

O'Dowd, C. D., Facchini, M. C., Cavalli, F., Ceburnis, D., Mircea, M., Decesari, S., Fuzzi, S., Yoon, Y. J., and Putaud, J.-P.: Biogenically driven organic contribution to marine aerosol, Nature, 431, 676–680, http://www.nature.com/nature/journal/v431/n7009/suppinfo/nature02959_S1.html, 2004.

Oliveira, C., Pio, C., Alves, C., Evtyugina, M., Santos, P., Gonçalves, V., Nunes, T., Silvestre, A. J. D., Palmgren, F., Wåhlin, P., and Harrad, S.: Seasonal distribution of polar organic compounds in the urban atmosphere of two large cities from the North and South of Europe, Atmos. Environ., 41, 5555–5570, http://dx.doi.org/10.1016/j.atmosenv.2007.03.001, 2007.

Oros, D. R. and Simoneit, B. R. T.: Identification and emission factors of molecular tracers in organic aerosols from biomass burning Part 2. Deciduous trees, Appl. Geochem., 16, 1545–1565, doi:10.1016/s0883-2927(01)00022-1, 2001.

Osthoff, H. D., Roberts, J. M., Ravishankara, A. R., Williams, E. J., Lerner, B. M., Sommariva, R., Bates, T. S., Coffman, D., Quinn, P. K., Dibb, J. E., Stark, H., Burkholder, J. B., Talukdar, R. K., Meagher, J., Fehsenfeld, F. C., and Brown, S. S.: High levels of nitryl chloride in the polluted subtropical marine boundary layer, Nat. Geosci., 1, 324–328, http://www.nature.com/ngeo/journal/v1/n5/suppinfo/ngeo177_S1.html, 2008.

Pavuluri, C. M., Kawamura, K., and Swaminathan, T.: Water-soluble organic carbon, dicarboxylic acids, ketoacids, and α -dicarbonyls in the tropical Indian aerosols, J. Geophys. Res., 115, D11302, doi:10.1029/2009jd012661, 2010.

Pechtl, S. and von Glasow, R.: Reactive chlorine in the marine boundary layer in the outflow of polluted continental air: A model study, Geophys. Res. Lett., 34, L11813, doi:10.1029/2007gl029761, 2007.

Perelygin, I. S. and Klimchuk, M. A.: Infrared spectra of coordinated acetone, J. Appl. Spectrosc., 20, 687–688, doi:10.1007/bf00607479, 1974.

Rudich, Y.: Laboratory Perspectives on the Chemical Transformations of Organic Matter in Atmospheric Particles, Chem. Rev., 103, 5097–5124, doi:10.1021/cr020508f, 2003.

Kundu, S., Kawamura, K., Andreae, T. W., Hoffer, A., and Andreae, M. O.: Molecular distributions of dicarboxylic acids, ketocarboxylic acids and $\alpha$-dicarbonyls in biomass burning aerosols: implications for photochemical production and degradation in smoke layers, Atmos. Chem. Phys., 10, 2209–2225, doi:10.5194/acp-10-2209-2010, 2010.

Schauer, J. J., Kleeman, M. J., Cass, G. R., and Simoneit, B. R. T.: Measurement of Emissions from Air Pollution Sources. 3. C1-C29 Organic Compounds from Fireplace Combustion of Wood, Environ. Sci. Technol., 35, 1716–1728, doi:10.1021/es001331e, 2001.

Schauer, J. J., Kleeman, M. J., Cass, G. R., and Simoneit, B. R.: Measurement of emissions from air pollution sources. 4. C1–C27 organic compounds from cooking with seed oils, Environ. Sci. Technol., 36, 567–575, 2002.

Sciare, J., Oikonomou, K., Favez, O., Liakakou, E., Markaki, Z., Cachier, H., and Mihalopoulos, N.: Long-term measurements of carbonaceous aerosols in the Eastern Mediterranean: evidence of long-range transport of biomass burning, Atmos. Chem. Phys., 8, 5551–5563, doi:10.5194/acp-8-5551-2008, 2008.



Singleton, D. L., Paraskevopoulos, G., and Irwin, R. S.: Rates and mechanism of the reactions of hydroxyl radicals with acetic, deuterated acetic, and propionic acids in the gas phase, J. Am. Chem. Soc., 111, 5248–5251, doi:10.1021/ja00196a035, 1989.

Smith, I. W. M. and Ravishankara, A. R.: Role of Hydrogen-Bonded Intermediates in the Bimolecular Reactions of the Hydroxyl Radical, J. Phys. Chem. A, 106, 4798–4807, doi:10.1021/jp014234w, 2002.

Smith, J. D., Kroll, J. H., Cappa, C. D., Che, D. L., Liu, C. L., Ahmed, M., Leone, S. R., Worsnop, D. R., and Wilson, K. R.: The heterogeneous reaction of hydroxyl radicals with sub-micron squalane particles: a model system for understanding the oxidative aging of ambient aerosols, Atmos. Chem. Phys., 9, 3209–3222, doi:10.5194/acp-9-3209-2009, 2009.

Spicer, C. W., Chapman, E. G., Finlayson-Pitts, B. J., Plastridge, R. A., Hubbe, J. M., Fast, J. D., and Berkowitz, C. M.: Unexpectedly high concentrations of molecular chlorine in coastal air, Nature, 394, 353–356, 1998.

Tervahattu, H., Hartonen, K., Kerminen, V.-M., Kupiainen, K., Aarnio, P., Koskentalo, T., Tuck, A. F., and Vaida, V.: New evidence of an organic layer on marine aerosols, J. Geophys. Res., 107, 4053, doi:10.1029/2000jd000282, 2002a.

Tervahattu, H., Juhanoja, J., and Kupiainen, K.: Identification of an organic coating on marine aerosol particles by TOF-SIMS, J. Geophys. Res., 107, 4319, doi:10.1029/2001jd001403, 2002b.

Tervahattu, H., Juhanoja, J., Vaida, V., Tuck, A. F., Niemi, J. V., Kupiainen, K., Kulmala, M., and Vehkamäki, H.: Fatty acids on continental sulfate aerosol particles, J. Geophys. Res., 110, D06207, doi:10.1029/2004jd005400, 2005.

Wang, G., Kawamura, K., Lee, S., Ho, K., and Cao, J.: Molecular, Seasonal, and Spatial Distributions of Organic Aerosols from Fourteen Chinese Cities, Environ. Sci. Technol., 40, 4619–4625, doi:10.1021/es060291x, 2006.

Wang, X., Luo, L., Ouyang, G., Lin, L., Tam, N. F. Y., Lan, C., and Luan, T.: One-step extraction and derivatization liquid-phase microextraction for the determination of chlorophenols by gas chromatography–mass spectrometry, J. Chromatogr. A, 1216, 6267–6273, doi:10.1016/j.chroma.2009.07.011, 2009.

Westervelt, D. M., Moore, R. H., Nenes, A., and Adams, P. J.: Effect of primary organic sea spray emissions on cloud condensation nuclei concentrations, Atmos. Chem. Phys., 12, 89–101, doi:10.5194/acp-12-89-2012, 2012.

Yoon, Y. J., Ceburnis, D., Cavalli, F., Jourdan, O., Putaud, J. P., Facchini, M. C., Decesari, S., Fuzzi, S., Sellegri, K., Jennings, S. G., and O'Dowd, C. D.: Seasonal characteristics of the physicochemical properties of North Atlantic marine atmospheric aerosols, J. Geophys. Res., 112, D04206, doi:10.1029/2005jd007044, 2007.

Yu, J., Flagan, R. C., and Seinfeld, J. H.: Identification of Products Containing-COOH, -OH, and -CO in Atmospheric Oxidation of Hydrocarbons, Environ. Sci. Technol., 32, 2357–2370, doi:10.1021/es980129x, 1998.

Zuo, Y., Zhang, K., and Lin, Y.: Microwave-accelerated derivatization for the simultaneous gas chromatographic-mass spectrometric analysis of natural and synthetic estrogenic steroids, J. Chromatogr. A, 1148, 211–218, doi:10.1016/j.chroma.2007.03.037, 2007.



**Table 1.** Summary of measured uptake coefficients for heterogeneous reaction systems involving organic aerosol with the radical species $OH^{\cdot}$ and $Cl^{\cdot}$.

| Uptake coefficient | OH | Cl |
|---|---|---|
| Squalane ($C_{30}H_{62}$) | $\gamma_{Sq}$ = 0.3 (Smith et al., 2009) | $\gamma_{Sq}$ = 3 in $N_2$ (Liu et al., 2011)<br>$\gamma_{Sq}$ = 0.6 in $N_2/O_2$ (Liu et al., 2011) |
| DOS ($(CH_2)_8(COOC_8H_{17})_2$) | $\gamma_{DOS}$ = 2.0 (Hearn and Smith, 2006) | $\gamma_{DOS}$ = 1.7 in $N_2/O_2$ (Hearn et al., 2007) |
| Palmitic acid ($C_{16}H_{32}O_2$) | $\gamma_{PA}$ = 0.3 (McNeill et al., 2008) | 0.1 $<\gamma_{Cl}<$ 1 in $N_2$ (Ciuraru, 2010)<br>$\gamma_{PA}$ = 14 ± 5 in $N_2$ (this work)<br>$\gamma_{PA}$ = 3 ± 1 in $N_2$ /$O_2$ (this work) |

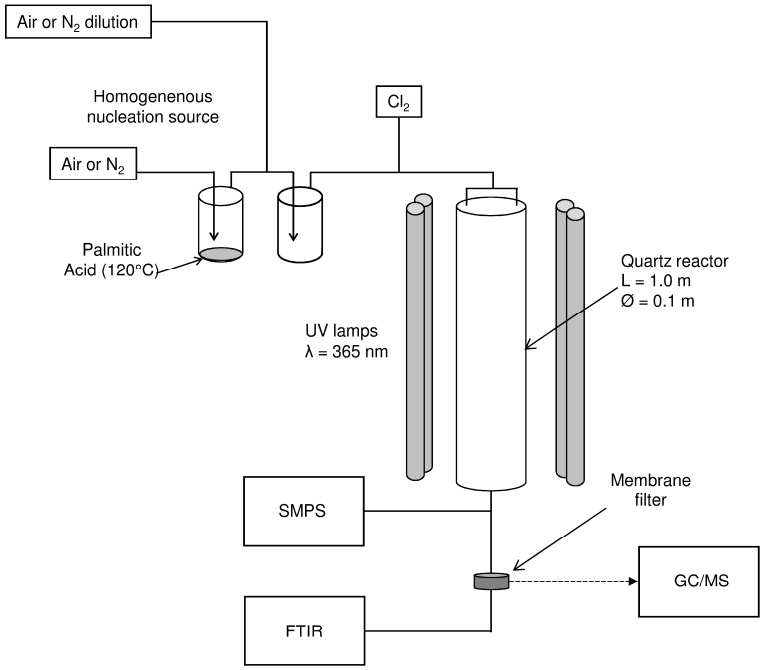


**Fig. 1.** Experimental setup, SMPS (Scanning Mobility Particle Sizer), FTIR (Fourier Transform InfraRed spectrometer), GC/MS (Gas Chromatography, Mass Spectrometer).



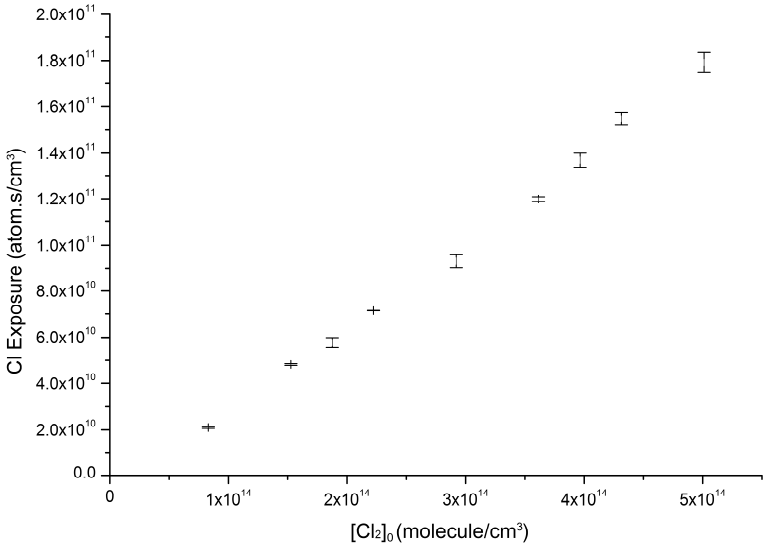


**Fig. 2.** Chlorine exposure as function of the initial $Cl_2$ concentration in the reactor; $Q_{tot}$ = 4.0 L min$^{-1}$ and 8 UV lamps powered. Errors bars express the minimum and maximum values of 4 experiments.

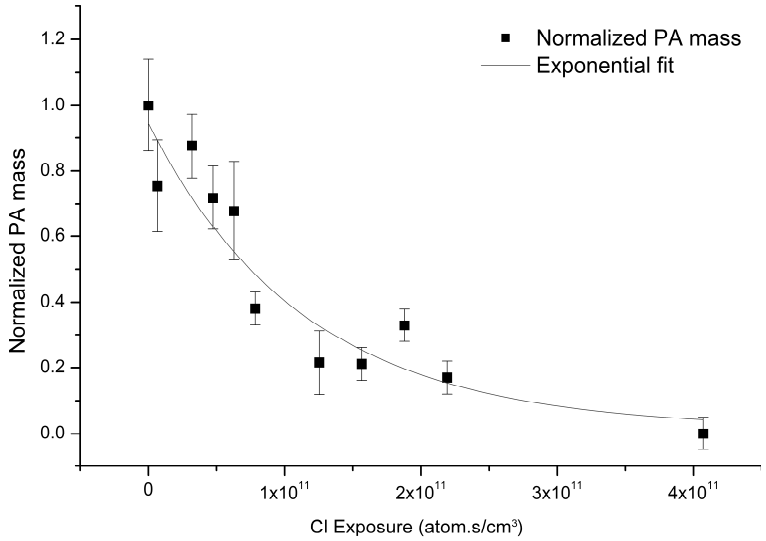


**Fig. 3.** Normalized mass of PA remaining in the particles collected on filter during 10 min as a function of the chlorine exposure (squares). Each data point is the mean value obtained from three GC/MS analyses of two particles samples. Errors bars represent the minimum and maximum values. The data have been fitted by an exponential function (solid line).



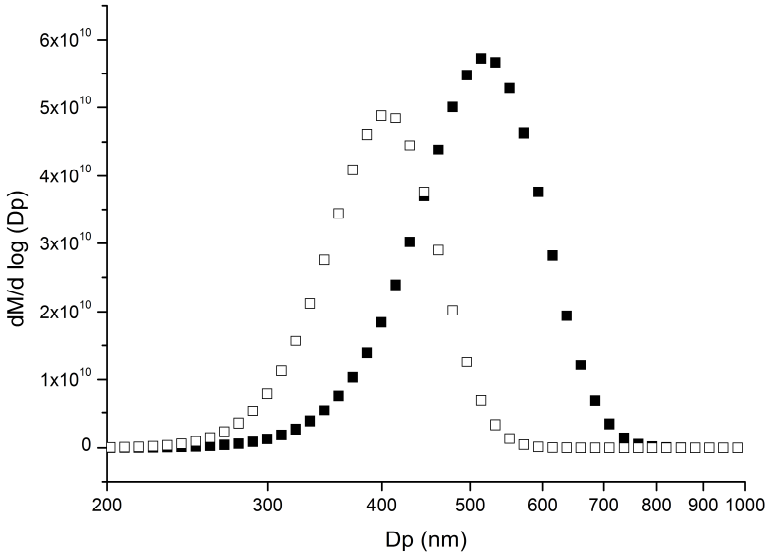


**Fig. 4.** Mass-weighted particle distribution (normalized $\mu g\,m^{-3}$) of PA particles before (filled squares) and after (open squares) a chlorine exposure of $1.25 \times 10^{11}$ atom $cm^{-3}$ s. Each distribution is the average of eight measurements.

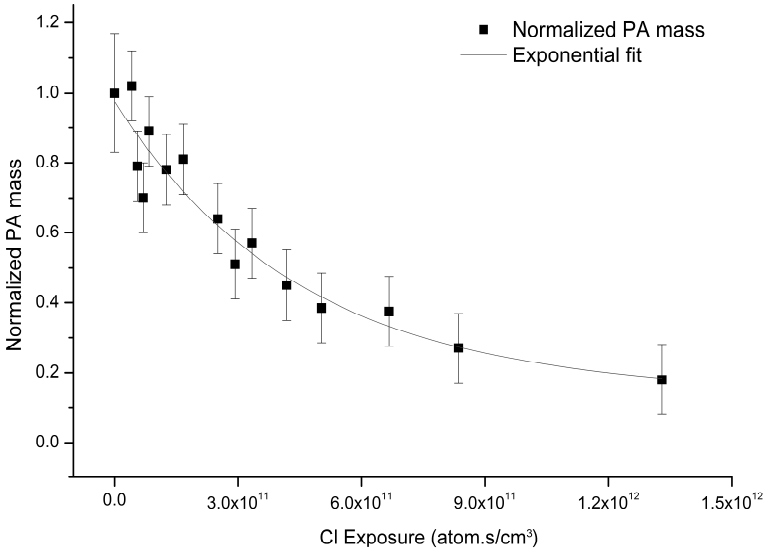


**Fig. 5.** Normalized mass of PA remaining in the particles as a function of the chlorine exposure in the presence of oxygen (squares) and the corresponding exponential fit (solid line).



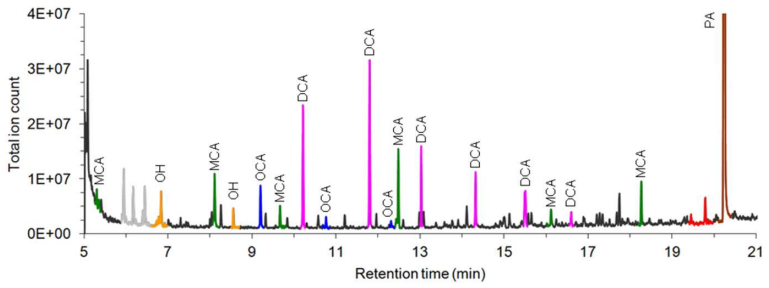


**Fig. 6.** Chromatogram of the sylilated-products from the Cl-initiated oxidation of PA in the presence of $O_2$. MCA peaks are monocarboxylic acids, OCA peaks are oxocarboxylic acids, DCA peaks are dicarboxylic acids, OH peaks are the alcohols, the PA peak is the remaining palmitic acid.

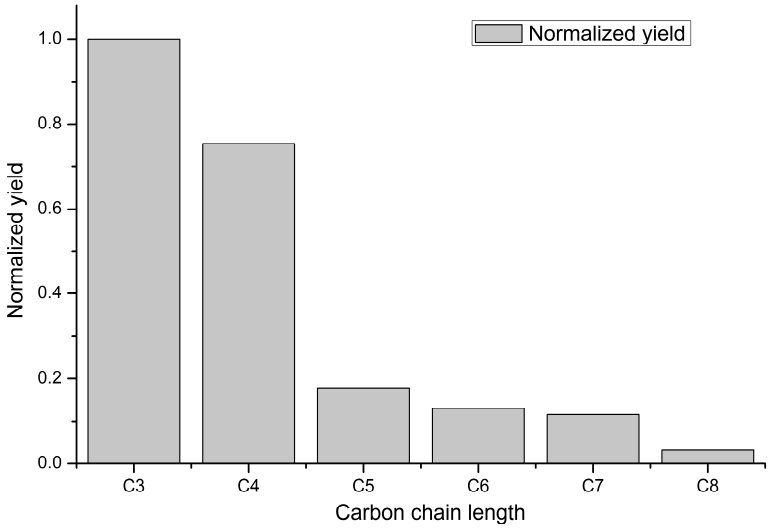


**Fig. 7.** Normalized yields of the detected dicarboxylic acids as function of the carbon chain length.



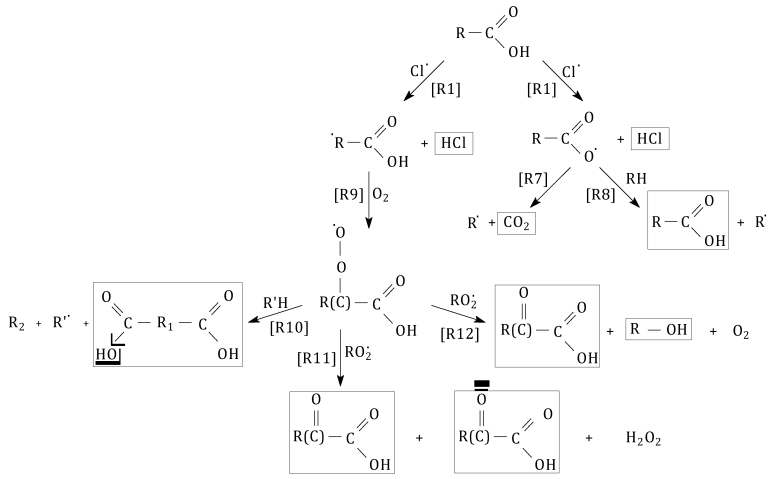


**Fig. 8.** Reaction mechanism for the chlorine radical initiated oxidation of palmitic acid in the presence of $O_2$. Observed products are framed.